International Journal of Environmental Science and Technology (2022) 19:6183–6200
https://doi.org/10.1007/s13762-022-03972-9

ORIGINAL PAPER

Treatability study of synthesized silica nanoparticles to reduce pollution load of industrial wastewater

K. U. Zaman[1] · N. Abbas[2] · M. Irshad[1] · S. Zehra[3] · M. T. Butt[2] · K. Shehzad[1] · H.-R. Mahmood[1]

Received: 7 December 2021 / Revised: 13 January 2022 / Accepted: 17 January 2022 / Published online: 9 February 2022

Abstract
Nanomaterials hold great potential to reduce pollution load from industrial wastewater. The silica nanoparticles (SNPs) were synthesized by sol–gel method and characterized by FTIR spectroscopy, XRD analysis and UV–visible spectroscopy. These SNPs were applied on industrial wastewater for reduction of pollution load, collected from Blund Dyestuff industry. To calculate treatment efficacy all parameters like color, total dissolve solids and conductivity were measured before and after treatment. Response surface methodology (RSM) was applied to design reaction layout for five groups of synthesized SNPs to evaluate the best among all. SNPs were also used in combination with natural coagulant; Potassium Aluminum Sulfate (alum) which boosted the activity of synthesized SNPs. It was observed that silica nanoparticles (SN-3) calcinated at 700 °C showed better results among the five types of SNPs. It reduced color up to 75%, conductivity 25% and TDS up to 35% at dose 0.16 g/100 ml of wastewater, 4 h contact time and 8 pH of original solution along with 8 mL of 10% alum solution. Other groups of SNPs showed reductions as well but lesser, as compared to SN-3.

Introduction

Industrial units play an important role in economy of a country but they have a troublesome side effect, production of effluents. These effluents including phenols, dyes, heavy metals, solid suspended wastes and different gases like hydrogen sulphide strictly damage the quality of water (Irfan et al. 2020). Many industries including textiles, rubber, leather, food, printing, paper and beverage industries use dyes as a coloring agent to color their product. In recent years, increasing demand and application of dyes in industries, has become a solemn environmental object due to discharged of dye effluent in wastewater from these industries (Ahmad and Ansari 2021).

Dyes in water channels are producing unimaginable chaos and posing serious threat to life. They remain in water for extended period of time because they are resistant to degradation and thermally stable (Gita et al. 2017). Therefore, novel and advanced methods for reducing pollution load of industrial wastewater must be implemented to protect our environment.

Nanoparticles, possessing remarkable properties, have applications in almost every field of life. Large surface area, catalytic potential, mobility and higher adsorption capacity make nanomaterials excellent adsorbents for the removal of aquatic effluents (Basu et al. 2015). Among multiple approaches employed so far for the removal of dyestuffs and other pollutants, adsorption has attracted much attention due to advantages such as high efficiency, ease of use, low energy consumption, and cost-effectiveness (Mittala et al. 2021). They are being analyzed in the field of diagnosis and therapy of cancer and for the treatment of other diseases like leukemia (Baetke et al. 2015; Soni and Yadav 2015). Nanoparticles have been found effective for their uses in industrial domains. They are believed to provide attractive chemical product design (Stark et al. 2015). Nanoparticles are being considered as multipurpose future prospective in various fields of life. They can do wonders in the fields of environment protection (Mohammed et al. 2017) synthesis of copolymers (Li et al. 2018), solar photo-catalysis Ong et al. 2018), anti-microbial activities (Ahmed et al. 2016), controlling infectious diseases (Zazo et al. 2016), In food industry for increased production of food and its packaging

Editorial responsibility: M Shabani.

✉ N. Abbas
naeemchemist@gmail.com

1 Department of Chemistry, University of Education, Lahore, Pakistan

2 Center for Environmental Protection Studies, PCSIR Laboratories Complex, Lahore, Pakistan

3 Mineral Processing Research Centre, PCSIR Laboratories Complex, Lahore, Pakistan

Graphical abstract

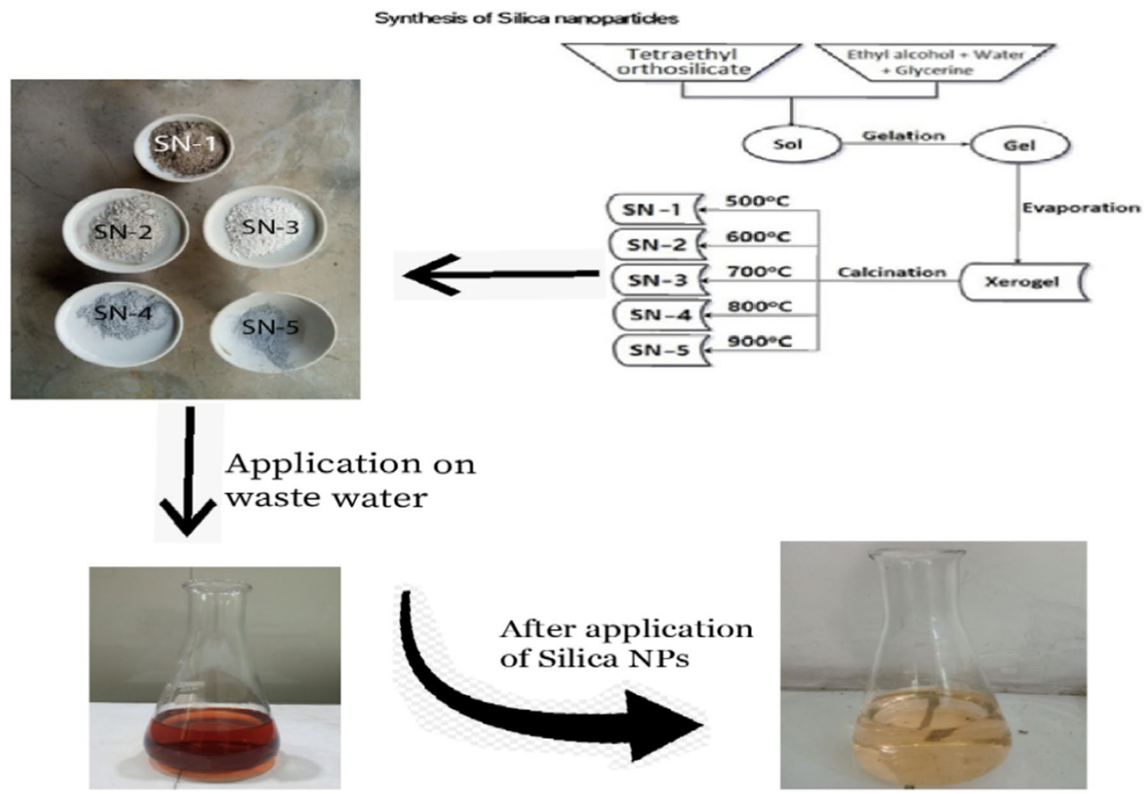

Keywords Silica nanoparticles · Sol Gel · Pollution load · Calcinated · Response surface methodology

and its protection (Ealias and Saravanakumar 2017), in magnetic devices and as oxidizing agent in thermite compensation Ali et al. 2016), in industrial motors, they are used as Ferro fluid which serves for damping (Ali et al. 2016); Ealias and Saravanakumar (2017).

Nanomaterials provide many possibilities for treatment of polluted water. They are used for the purification of industrial wastewater through several methods such as photo-catalysis, nano sorbents and adsorption. These methods when modified in some way or the other, present greater efficiency. Conventional methods for the treatment of wastewater include coagulation flocculation process, reverse osmosis, and filtration. These techniques, however, are not efficient in removing all the pollutants more effectively. Therefore, there is need for more advanced techniques for water purification (Khan et al. 2019).

In recent years, nanoparticles and more specifically SNPs have attracted a good deal of attention in water treatment process. They hold great importance in environmental remediation operations. Owing to their versatile chemical and physical characteristics, they have been efficiently used for removal of heavy metals like arsenic, lead, mercury from contaminated water. SNPs have been coated with different metals for certain objectives as well (Attinti et al. 2015). They have been found effective in removing carcinogenic radioactive elements like uranium and thorium from aquatic media. They have also been used as careers in drug delivery systems specifically for anticancer drugs (Zhu and Liao 2015). Conventional methods for purification of wastewater include reverse osmosis, ion exchange, precipitation and chemical absorbents. Sustainable technologies, despite all developments, however, are disadvantageous as they have high cost, less efficiency and poor recyclability. Uses of nanomaterials have proved that it can offer more reliability in wastewater treatment process on bulk scale (Singh et al. 2019). Carbon encapsulated iron nanoparticles have successfully been reported for their efficient use against removal of methylene blue, phenols and Congo-red (Zhang 2011). Polyethersulfone membranes which are used for ultrafiltration have been removed by using aluminum oxide and zirconium oxide nanoparticles in order to avoid membrane fouling (Heidi Lynn et al. 2012). Zinc oxide nanoparticles owing to remarkable photocatalytic activity, have been used broadly in wastewater treatment processes. Nanoparticles of silica, copper and titanium were also found effective in water treatment processes specially against microbial activities (Naseem and Durrani 2021). Silica nanoparticles possess great potential for absorbing effluents from wastewater.

It was reported that silica modified with cyclodextrin has shown efficient removal of organic and inorganic pollutants from aqueous solutions (Morin-Crini 2019). Magnetite doped silica-ionic liquids were also found potent for their absorbance of dyes from wastewater (Atta 2020).

Nanoparticles are synthesized by different methods. Every method gives different size, shape, porosity and morphology to the nanoparticles. During the formation the exposure to oxygen result in the formation of metal oxide nanoparticles. They possess extra properties than their respective metals (Ealias and Saravanakumar 2017). A few of them are sol–gel method, mechanical milling, thermal decomposition, and laser ablation.

In current research work, synthesized SNPs were divided into five groups based on difference in their calcination temperature. These SNPs were characterized by FTIR, UV spectroscopy and XRD. It was amid that which group of nanoparticles reduces the pollution load of industrial wastewater more efficiently.

Materials and methods

Synthesis of silica (SiO_2) nanoparticles

Silica nanoparticles (SNPs) were prepared by sol–gel method as reported by (Prasad et al. 2020), one of the most commonly used technique in preparation of ultra-fine materials (Ramimoghadam et al. 2014). Tetra ethyl ortho silicate (TEOS) was used as precursor salt for the synthesis of SNPs. 2-ethyl hexanol was used as solvent for production of alkoxide and then a suitable quantity of ethanol was added to it. Glycerin was used as a reducing agent.

At first 20 mL of TEOS was taken in a beaker along with hexanol and glycerin. The whole mixture was stirred for 30 minutes. After this initial stirring, 10 mL of absolute ethanol was added and again stirred on magnetic stirrer for 1 h. The pH of the reaction mixture was maintained at 2. A sol was obtained which was left for evaporation to get a gel overnight. A gel was obtained which was further evaporated at 70 °C for 3 hours to evaporate water and other volatile organic compounds. This treatment gave us a dry xerogel. It was further separated by centrifugation. Freshly prepared nanoparticles were taken in centrifuge tubes which were placed in the centrifuge machine and were run at 6000 rounds per minutes for thirty minutes until the silicon dioxide nanoparticle settled at the bottom of the centrifuge tubes which were then separated. After centrifugation the sample obtained was divided into five groups and each of five samples was calcinated at different temperatures. The sample 1 was given the name SN-1 and it was calcinated at 500 °C in the furnace and other samples named SN-2, SN-3, SN-4 and SN-5 were calcinated at 600 °C, 700 °C, 800 °C and 900 °C, respectively. It was desired to check the effect of calcination temperature on the absorptive activity of SNPs. The calcinated products were grounded to fine powder with the help of pestle and mortar. The off white and greyish colored powder was stored, and characterization was done Table 1 and Fig. 1.

Characterization of Silica Nanoparticles (SNPs)

Chemically synthesized SNPs were characterized by FTIR spectroscopy for knowing purity of the nano powder, XRD analysis for determination of crystal or amorphous structure and UV–visible spectroscopy for identification of SNPs.

Surface properties of SNPs

FTIR technique is used to get the IR spectrum of transmission or absorbance of different compounds in the samples. Depending on the infrared absorption frequency range 600–4000 cm^{-1}, the specific functional groups present in the sample can be identified through spectrum data in the automated software (Mohammadi et al. 2019). FTIR helps in characterization of synthesized compounds by comparing obtained data with literature values.

X-Ray Diffraction (XRD) Analysis

XRD analysis uses X-rays for identification crystal phase structure of target compound. It was used to explore the crystalline structure, lattice parameters, crystalline grain size and amorphous phase structure of SNPs (Mourdikoudis et al. 2018).

UV–Visible Spectroscopy

The effect of particle size on electronic absorption behavior was studied by using UV–Vis spectrophotometer (Stanley and Nesaraj 2014). Ultraviolet spectroscopy provides valuable information about the presence of desired compound in sample (Rovani et al. 2018).

Application of SNPs on wastewater

SNPs were evaluated for reducing pollution load (Color, Conductivity and Total dissolved solids) of industrial wastewater. For this purpose, wastewater was taken from Blund Dyestuff industry located on Mandi-Bahauddin Road, Lahore. Blund Dyestuff is food color manufacturing industry and SNPs were applied on dye effluent water from this industry for their evaluation. The collected sample of wastewater was stored in plastic gallon at room temperature. The raw characterization of wastewater given in Table 2 was done in the Center for Environmental Protection Studies (CEPS), PCSIR laboratories complex, Lahore.

Before starting experimental work on industrial wastewater, raw analysis was performed. It was desired to make these necessary initial measurements in order to check the nature of sample and to design possible treatments solution accordingly All parameters of sample under investigation were compared with National Environmental Quality Standards (NEQS) for municipal and liquid industrial effluents.

Formation of solutions on the basis of pH

At first the 20% solution of industrial wastewater was taken and was divided into three groups on the basis of pH so that we may check that at which pH SNPs show maximum reduction of pollution load. These values of pH were: 7, 8 and 9. To maintain the pH, 10% HCl and 10% NaOH solutions were used. 10% solution of natural coagulant alum was also utilized along with SNPs.

Batch experiment

Trail reactions were performed in order to assess the activity of SNPs on wastewater. In some reactions sole SNPs were applied to wastewater, in others, SNPs were combined with alum solution. Effect of pH was also observed on activity of SNPs. Among these Bach experiments, it was discerned that reaction performed by taking 50 mL of 20% dilute original wastewater in 250 mL flask with 0.02 g of SNPs along with 4 mL of 10% solution of Potassium Aluminum Sulfate (alum) showed more reduction in color, conductivity and TDS. After these initial batch experiments optimization of parameters was performed.

Table 1 Classification of silica nanoparticles on the basis of calcination temperature

SN-1	SNPs calcinated at 500 °C
SN-2	SNPs calcinated at 600 °C
SN-3	SNPs calcinated at 700 °C
SN-4	SNPs calcinated at 800 °C
SN-5	SNPs calcinated at 900 °C

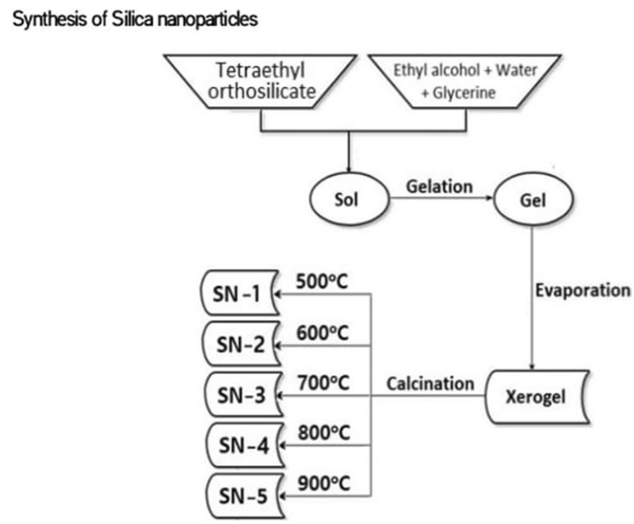

Fig. 1 Schematic representation of synthesis of SNPs

Table 2 Raw analysis of wastewater taken from Blund Dyestuff industry before applying SNPs

Parameter	Unit	Value	NEQS
pH	–	7 ± 0.7	6.5–9.5
Conductivity	mS/cm	609 ± 4	–
Turbidity	NTU	48.1 ± 2.7	–
Color	Pt–Co	21,800 ± 30	–
TDS	mg/L	251,207 ± 40	3500

Optimization

For optimizing dose of nanoparticles, alum, pH and contact time, design expert version 7.0.0 software was used, commonly known as response surface methodology.

Response surface methodology

The response surface methodology (RSM) is a statistical tool generally used for modeling and analyzing a process in which the response of interest is affected by various variables under investigation. The objective of this technique is to optimize the response (Xu et al. 2013). RSM reveals information and relative correlation between different parameters and the responses. RSM helps to generate knowledge about the experimental domain of interest (Baş and Boyacı 2007). It provides reliable estimate of variability (pure error) of experimental work. It not only guarantees the adequacy between experimental data and proposed model (helps to detect the lack of fit) but also helps in predicting observed responses as precisely and exactly as possible in those points in experimental domains where experiments are not performed.

In this study, it was aimed to examine that which variable effect the activity of SNPs the most among contact time, pH of the wastewater, silica dose rate, and quantity of alum solution.

Parameters used

Four process factors were analyzed through central composite design with their numeric range given in Table 3.

The effect of these process factors was observed on three responses to optimize conditions. These responses were: color, conductivity and TDS.

An experimental layout was obtained, and further batch reactions were performed according to it. Reaction layouts were obtained for all five types of nanoparticles. Experimental work was performed, and results were analyzed. It was observed that SN-3 showed the best results among all.

Table 3 Different parameters used in research work along with their ranges

Parameter	Unit	− 1 level	+1 level	− alpha	+alpha
Silica	Gram	0.02	0.08	0.01	0.11
pH	–	7	8	6.5	8.5
Time	Hours	1	4	0.5	5.5
Alum	mL	4	8	2	10

Results and discussion

SNPs were synthesized by sol–gel method calcinated at different temperatures. Sample 1 was given the name SN-1, it was calcinated at 500 °C and other samples named SN-2, SN-3, SN-4 and SN-5 were calcinated at 600 °C, 700 °C, 800 °C and 900 °C, respectively. These SNPs were characterized by FTIR spectroscopy, UV–visible spectroscopy and XRD analysis. After performing batch experiments, optimization of parameters was accomplished by using RSM. It was observed that SN-3 among all SNPs showed better results.

Surface properties of SNPs

The FTIR spectra of SN-1, SN-2, SN-3, SN-4 and SN-5 were recorded in the range of 1000–3500 cm^{-1}. All of these SNPs showed clear and sharp peaks at (a) 1073.01 cm^{-1}, (b) 1079.41 cm^{-1}, (c) 1072.68 cm^{-1}, (d) 1077.18 cm^{-1} and (e) 1077.63 cm^{-1}, respectively, and are presented in Fig. 4 which are close to standard SNPs (Prasad et al. 2020). The peaks in region of 1073–1079 cm^{-1} are assigned to asymmetric stretching vibrations of Si–O-Si. The peak at 799 cm^{-1} assigned to the Si–O-Si stretching vibration mode Xue et al. (2015).

X-ray Diffraction (XRD) Analysis

X-ray diffraction analysis was performed to explore the chemical nature and amorphous or crystalline phase structure of SNPs (SN-1, SN-2, SN-3, SN-4 and SN-5 calcinated at 500 °C, 600 °C, 700 °C, 800 °C and 900 °C, respectively). Obtained diffractograms are shown in Fig. 2. It is interpreted that SNPs calcinated at low temperature show amorphous structure while crystalline α-cristobalite structures were obtained at higher temperature. Characteristic peaks in Fig. 3 at 21.52°, 26.68°, 30.92° corresponding to spacing of 84, 69, 66 for SN-5 are quite close to the JCPDS PDF No. 39–1425 as reported in literature, whereas peak at 18.28° with spacing 35 in SN-1 corresponds to the quartz structure of silica which is close to JCPDS PDF No. 46–1045 as reported by (Wyckoff (Wyckoff 1925)). It was observed that extent of crystallization improved significantly by increase in temperature. Amorphous phase silica started phase transformation to crystalline α-cristobalite at near 700 °C with complete transformation at 900 °C in SN-5. These observations were in close agreement with previous studies Xue et al. (2015). A typical broad peak in XRD pattern at around 25 ° at 2θ position indicates the presence of SNPs (Nandanwar et al. 2015). As there are no other peaks which indicate high purity samples.

From these observations, it can be deduced that below 700 °C SNPs exist in amorphous phase hence SN-1 and SN-2 are amorphous. SN-3 predominantly a mixture of both amorphous and α-cristobalite whereas SN-4 and SN-5 are majorly crystalline in structure. Calcination at lower temperatures leads to the formation of amorphous phase while crystalline phase is reported to exist at higher calcination temperature (Bettermann and Liebau 1975).

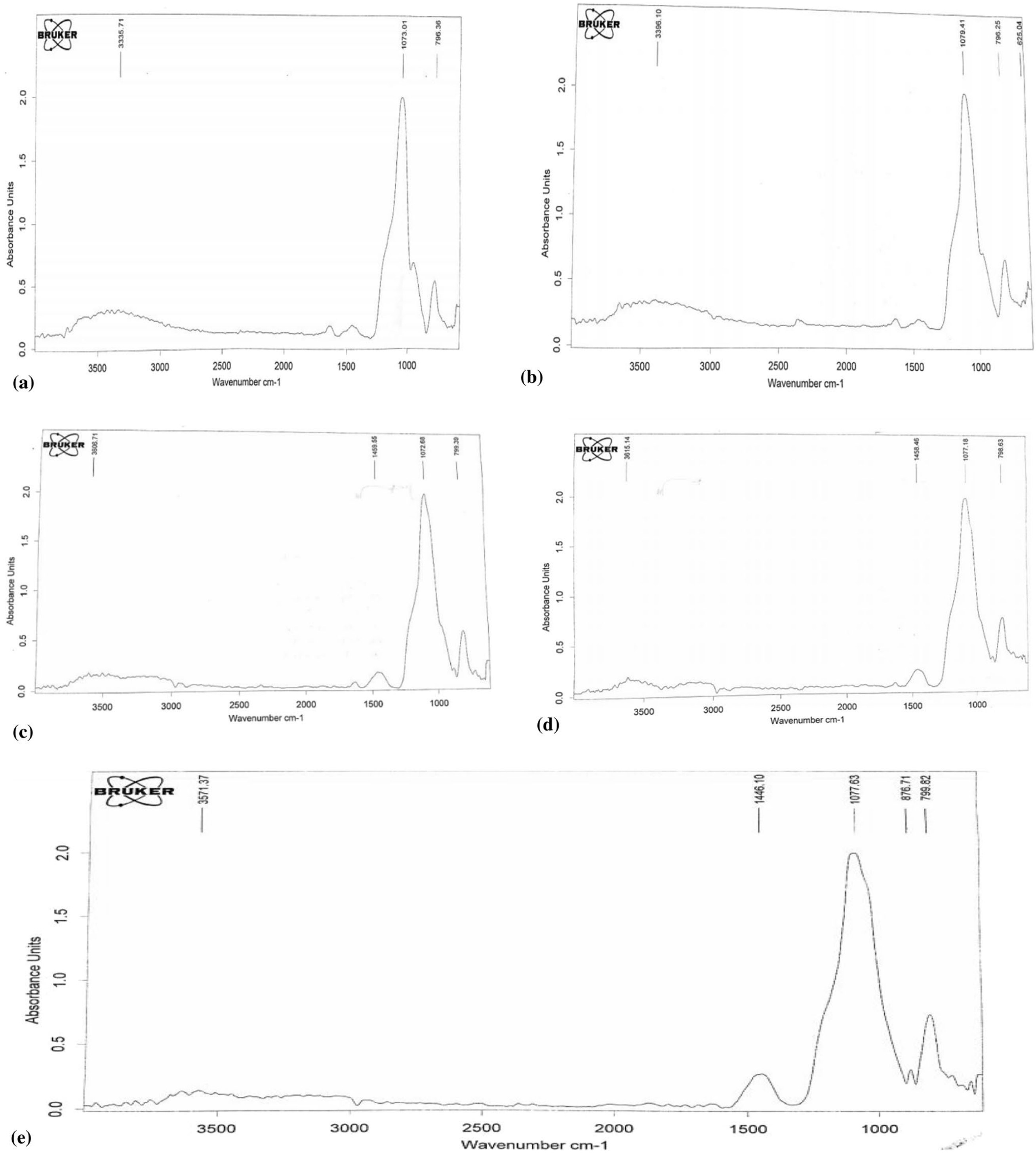

Fig. 2 FTIR spectra of **a** SN-1, **b** SN-2, **c** SN-3, **d** SN-4 and **e** SN-5

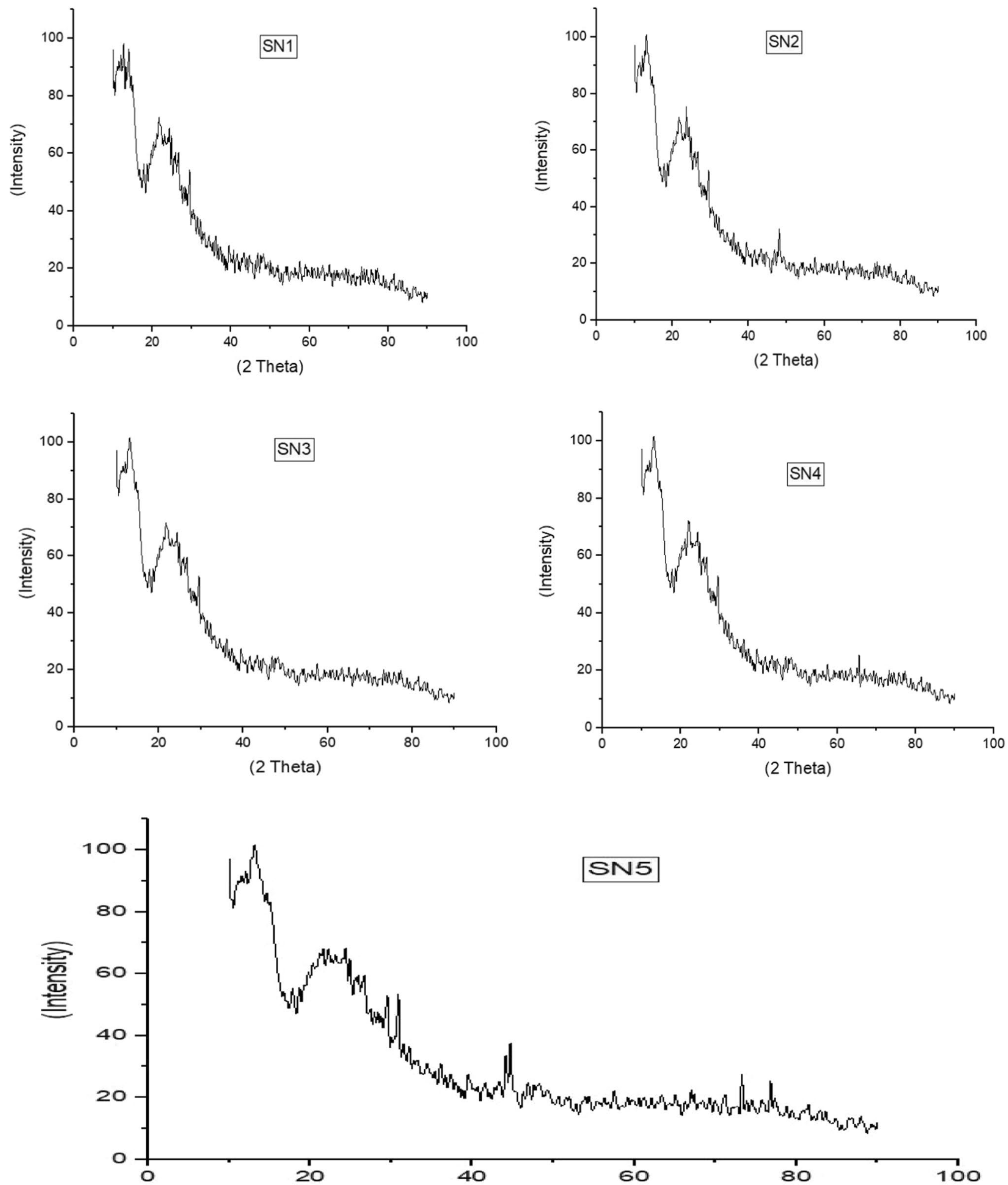

Fig. 3 XRD graph for SN-1, SN-2, SN-3, SN-4 and SN-5

UV–Visible spectroscopy

The effect of particle size on electronic absorption behavior of SNPs was determined by UV–Vis spectrophotometer. Ultraviolet spectroscopy provided valuable information about the presence of SNPs. UV–Vis absorption spectra of different particle sizes manifested a single ʎ max at (a) 482 nm, (b) 476 nm, (c) 474 nm, (d) 483 nm and (e) 480 nm shown in Fig. 4 which are close to literature value Kandpal et al. (2007).

Application of SNPs for reduction of pollution load

The reaction layouts for SN-1, SN-2, SN-3, SN-4 and SN-5 were obtained from design expert software. According to layout, set of 30 reactions were performed for each SNPs group with given variables and results of reduction in color, conductivity, and TDS were noted. All five groups of SNPs were applied separately, and results were measured. However, SN-3 showed better results as described in Table 4.

Reduction in color

Reduction in color of wastewater was observed through analysis provided by RSM as quadratic model was aliased as shown in Table 5.

ANOVA for response surface quadratic model for color

ANOVA is a statistic tool which help us to recognize that which factors are significant (have considerable effect on the response) and which factors are insignificant Olawale and Olawale (2012).

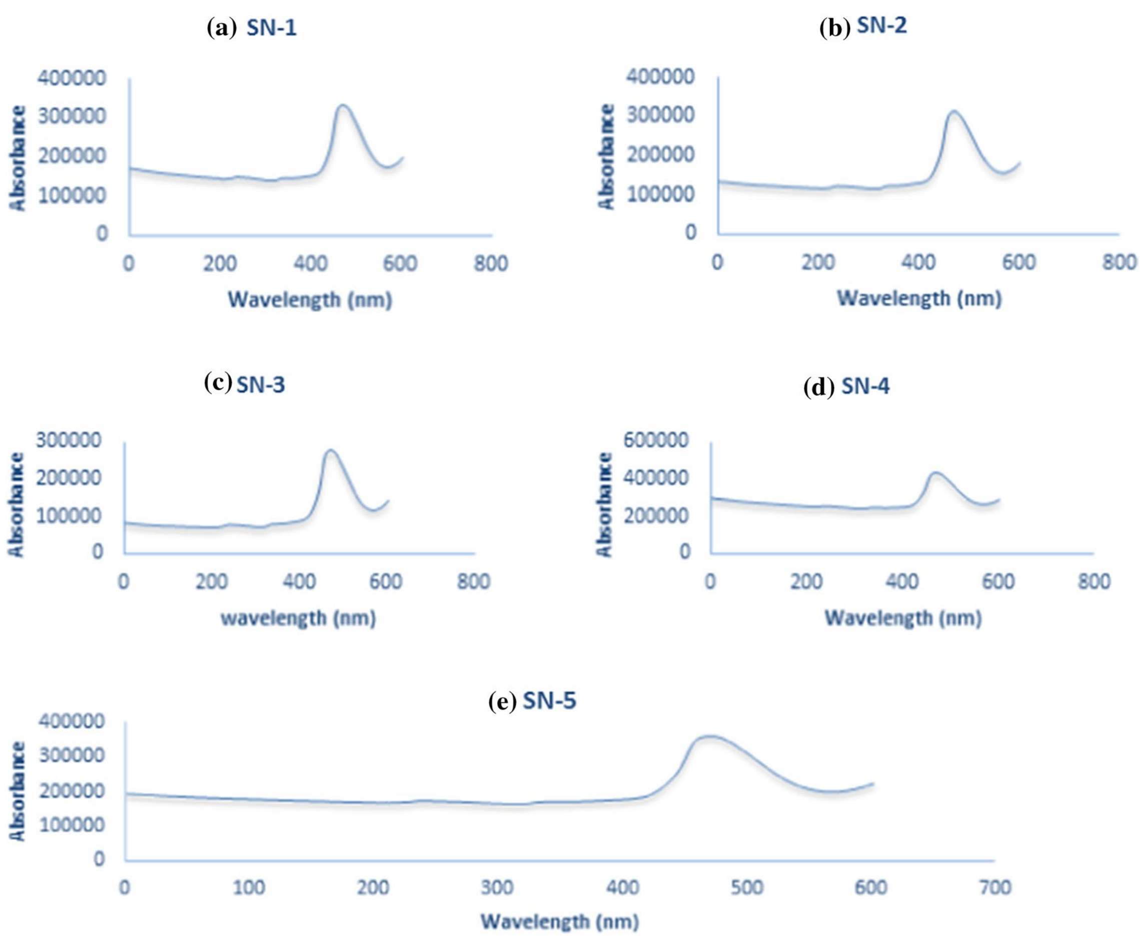

Fig. 4 UV spectra of **a** SN-1, **b** SN-2, **c** SN-3 **d** SN-4 and **e** SN-5. All showing sharp absorbance peaks

Table 4 Reactions layout

Std	Run	SNPs (g)	pH	Contact time (h)	Alum sol. (mL)	Response 1 Color (Pt–Co/Hazen)	Response 2 conductivity mS	Response 3 TDS
1	20	0.02	6	1	4	484	18.92	11.35
2	13	0.06	6	1	4	396	19.02	11.412
3	17	0.02	8	1	4	501	18.65	11.19
4	6	0.06	8	1	4	419	19.15	11.49
5	10	0.02	6	4	4	361	19.62	11.7
6	23	0.06	6	4	4	522	18.76	11.25
7	24	0.02	8	4	4	446	18.28	10.97
8	11	0.06	8	4	4	524	21.8	13.08
9	28	0.02	6	1	8	361	21.2	12.72
10	2	0.06	6	1	8	501	22.9	13.74
11	21	0.02	8	1	8	492	23.7	14.22
12	5	0.06	8	1	8	462	25.2	15.12
13	15	0.02	6	4	8	468	23.9	14.34
14	1	0.06	6	4	8	516	19.69	11.814
15	12	0.02	8	4	8	524	21.4	12.84
16	14	0.06	8	4	8	560	22.6	13.56
17	29	0.00	7	2.5	6	504	19.18	11.508
18	26	0.08	7	2.5	6	270	19.3	11.58
19	19	0.04	5	2.5	6	508	19.2	11.52
20	3	0.04	9	2.5	6	640	19.6	11.76
21	16	0.04	7	0.5	6	560	19.5	11.7
22	7	0.04	7	5.5	6	558	19.5	11.7
23	22	0.04	7	2.5	2	552	16.4	9.84
24	25	0.04	7	2.5	10	548	21.3	12.78
25	9	0.04	7	2.5	6	486	19.38	11.628
26	30	0.04	7	2.5	6	469	19.95	11.97
27	27	0.04	7	2.5	6	462	19.4	11.64
28	18	0.04	7	2.5	6	486	19.42	11.652
29	4	0.04	7	2.5	6	469	19.9	11.94
30	8	0.04	7	2.5	6	466	19.92	11.952

Table 5 Sequential model sum of squares, which predicts mean model as suggested and quadratic model as aliased

Source	Sum of Squares	Df	Mean square	F value	*P* value > F	Suggested / Aliased
Total vs Mean	7,022,841	1	7,022,841			Suggested
Mean vs Linear	21,760.17	4	5440.042	1.070183	0.3921	Aliased
Linear vs 2FI	17,265.38	6	2877.563	0.497863	0.8021	
Quadratic vs 2FI	46,882.21	4	11,720.55	2.793516	0.0646	Suggested
Quadratic vs Cubic	47,080.33	8	5885.042	2.598403	0.1129	Aliased
Residual	15,854.08	7	2264.869			
Total	7,171,683	30	239,056.1			

Table 6 Analysis of variance

Source	Sum of squares	Df	Mean square	F value	P value > F	Significant/ Not- significant
Model	1.531E+005	14	10,935.88	3.12	0.0181	Significant
A-SNPs	37,209.37	1	37,209.37	10.62	0.0053	
B-	14,162.04	1	14,162.04	4.04	0.0627	
C-Contact time	3775.04	1	3775.04	1.08	0.0158	
D-Alum sol	2072.04	1	2072.04	0.59	0.0439	
AB	4192.56	1	4192.56	1.20	0.0213	
AC	9168.06	1	9168.06	2.62	0.0266	
AD	976.56	1	976.56	0.28	0.0453	
BC	189.06	1	189.06	0.054	0.0195	
BD	264.06	1	264.06	0.075	0.0874	
CD	2475.06	1	2475.06	0.71	0.0139	
A^2	44,735.50	1	44,735.50	12.77	0.0028	
B^2	10,687.57	1	10,687.57	3.05	0.0124	
C^2	7012.57	1	7012.57	2.00	0.0176	
D^2	5177.86	1	5177.86	1.48	0.0240	
Residual	52,567.58	15	3504.51			
Lack of fit	52,027.58	10	5202.76			Not significant
Pure error	540.00	5	108.00	48.17	0.0002	
Cor total	2.057E+005	29				

The "Model F-value" of 1.46 in Table 6 suggests that the current model is significant relative to the noise. There is a 23.68% probability that a "Model F-value" this large could occur due to noise. Values of "Prob > F" less than 0.0500 indicate model terms are significant. In this case A2 are significant model terms. Values greater than 0.10 indicate the model terms are insignificant (Merci 2020) Table 7.

The final equations in terms of coded and actual factors for color reduction are given Eq. 1 & 2, respectively.

Table 7 Predicted and adjusted R-squared

Std. Dev.	59.20	R-squared	0.7444
Mean	480.27	Adj R-squared	0.5059
C. V %	12.33	Pred.R-squared	0.609
Press	3.005E+005	Adeq Precision	8.848

Equation in Terms of Coded Factors:

$$\begin{aligned} Color = &+ 473.00 + 39.37 * A + 24.29 * B \\ &+ 12.54 * C + 9.29 * D - 16.19 * A * B \\ &+ 23.94 * A * C + 7.81 * A * D + 3.44 * B * C \\ &+ 4.06 * B * D + 12.44 * C * D - 40.39 * A2 \\ &+ 19.74 * B2 + 15.99 * C2 + 13.74 * D2 \end{aligned} \tag{1}$$

Equation in Terms of Actual Factors:

$$\begin{aligned} Color = &+ 1236.84606 + 12544.79167 * SNPs \\ &- 237.60417 * pH - 100.00463 * contact\ time \\ &- 8.96875 * Alum - 809.37500 * SNPs * pH \\ &+ 797.91667 * SNPs * contact\ time \\ &+ 195.31250 * SNPs * Alum \\ &+ 2.29167 * pH * contact\ time \\ &+ 2.03125 * pH * Alum \\ &+ 4.14583 * contact\ time * Alum \\ &- 1.00964E + 005 * SNPs^2 + 19.73958 * pH^2 \\ &+ 7.10648 * contact\ time^2 + 3.43490 * Alum^2 \end{aligned} \tag{2}$$

Model graphs

3D surface and contour graph in Fig. 5 shows relative effect of SNPs and pH on color reduction of wastewater. The graph shows that maximum color reduction is obtained at 0.06 g of SNPs at pH nearly 7. Color reduction is minimum at least silica dose and higher pH. If dose rate is kept at 0.02–0.04 g, the color reduction is not much significant even at higher (more basic) pH.

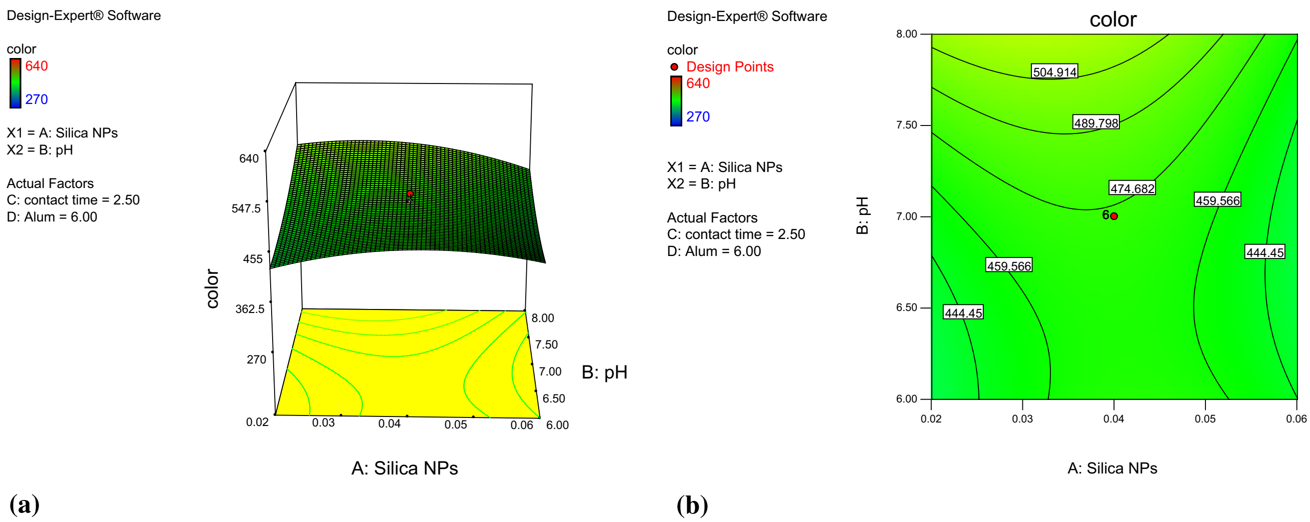

Fig. 5 **a** 3D surface and **b** contour graph, for relative outcome of SNPs and pH on color reduction

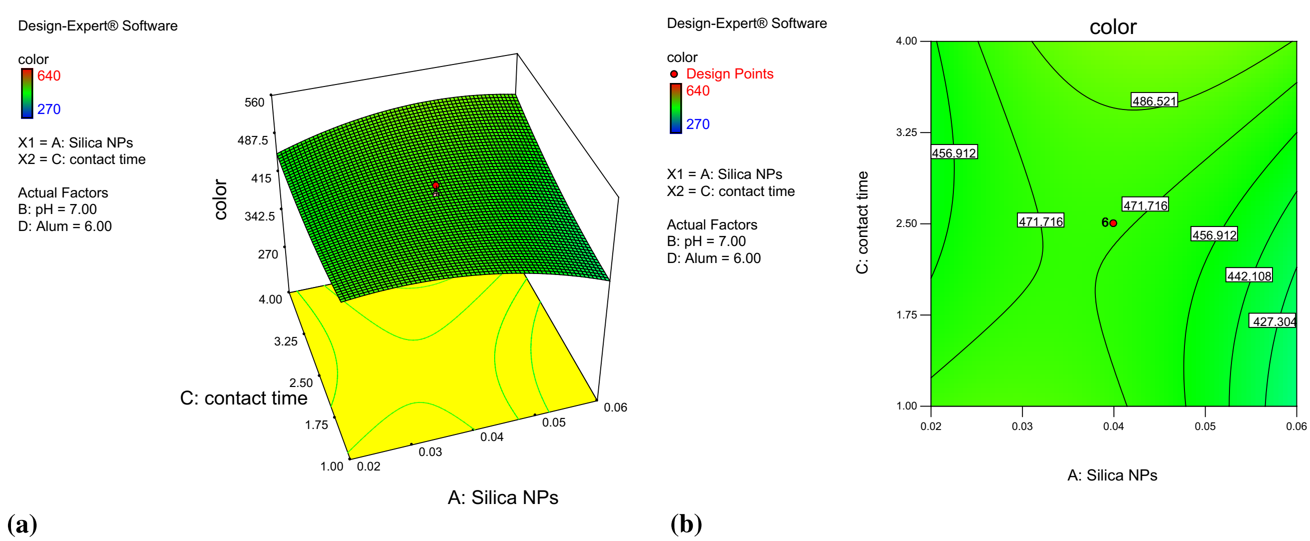

Fig. 6 **a** 3D surface and **b** contour graph, for relative sequel of SNPs and contact time on color reduction

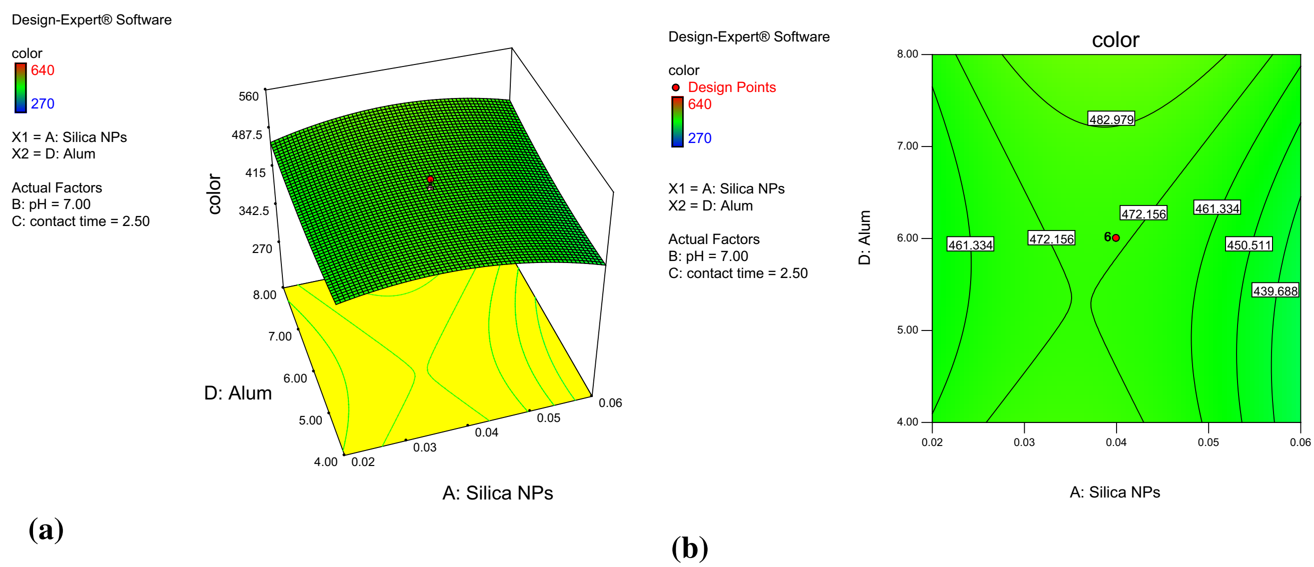

Fig. 7 **a** 3D surface and **b** contour graph, for relative effect of SNPs and alum solution on color reduction

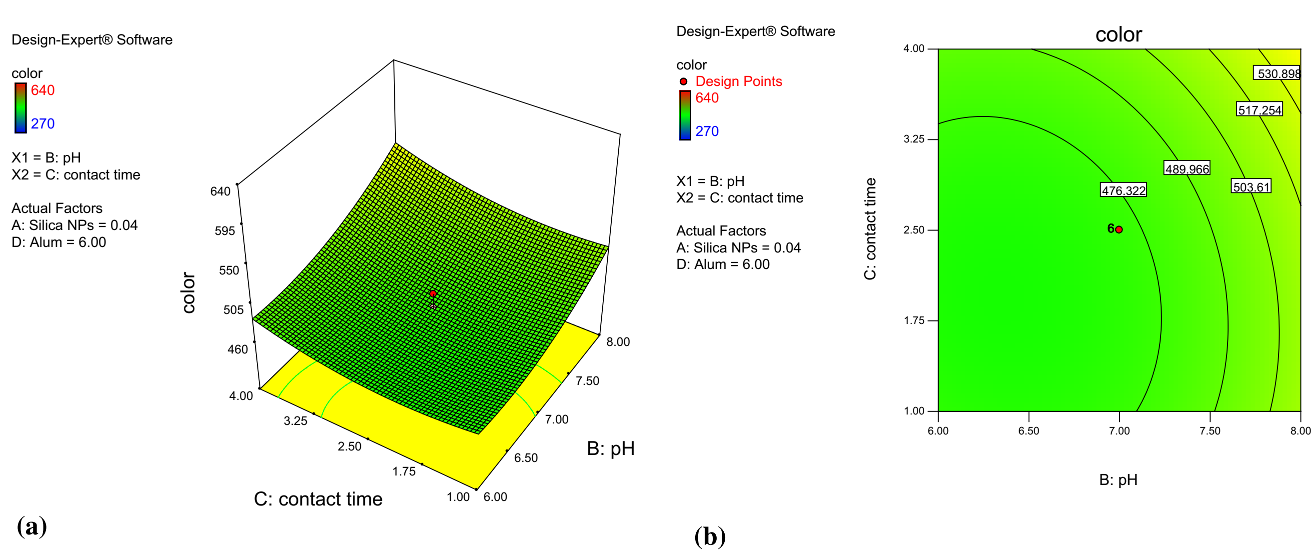

Fig. 8 **a** 3D surface and **b** contour graph, for relative effect of contact time and pH on color reduction

The 3D surface and contour graph for relative effect of SNPs and contact time on color reduction of wastewater is shown in Fig. 6. It is evident from contour that color reduction is minimum at lower silica dose with respect to time of 2-3 h. However, more time with higher silica dose show more reduction in color. It can be summed up that color reduction is independent of contact time with respect to silica dose rate.

The results shown in Fig. 7 demonstrate 3D surface and contour graph for relative effect of SNPs and alum solution on color reduction of wastewater. These two variables show a complex pattern regarding color reduction. Higher silica dose and 5–6 mL of 10% alum solution show more reduction in color. Increase in quantity of alum solution increases color reduction; however, silica dose is more effective variable.

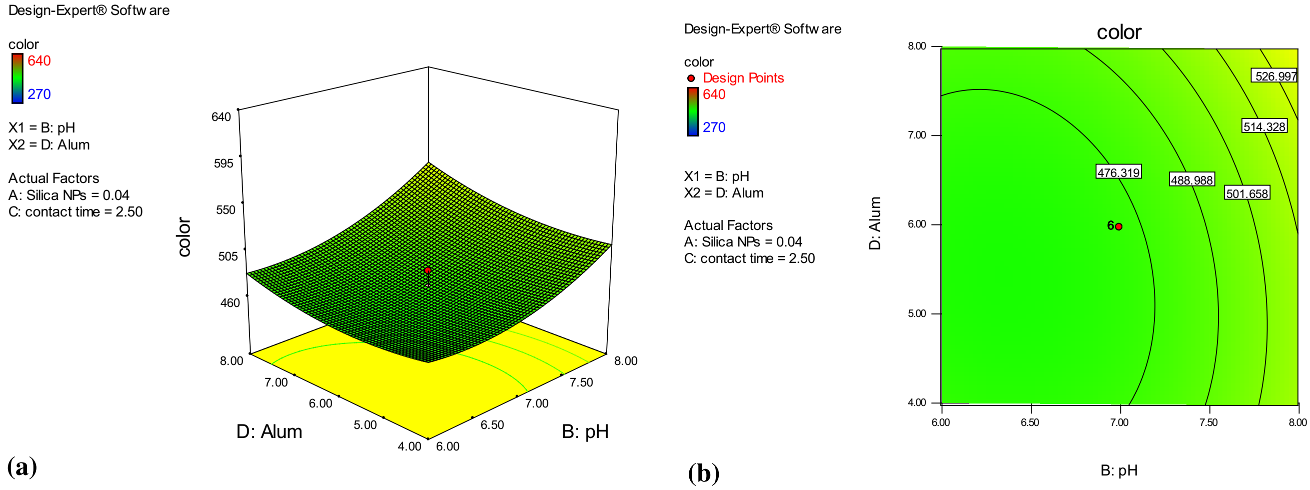

Fig. 9 **a** 3D surface and **b** contour graph, for relative outcome of pH and alum solution on color reduction 6

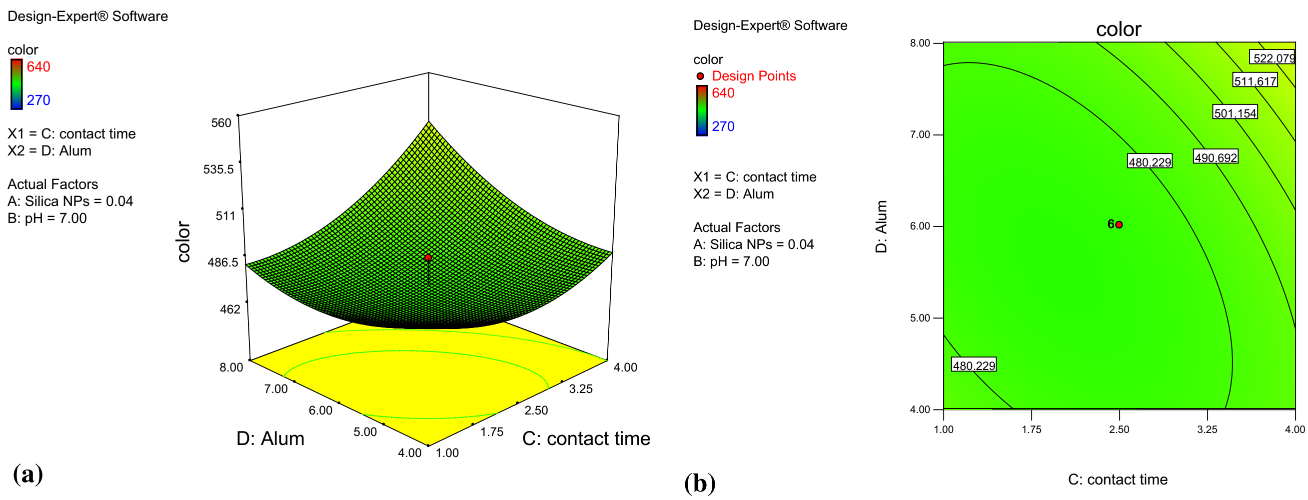

Fig. 10 **a** 3D surface and **b** contour graph, for relative effect of contact time and alum solution on color reduction

Table 8 Sequential model sum of squares for conductivity, which predicts mean model as suggested and quadratic model as aliased

Source	Sum of squares	Df	Mean square	F value	*P* value > F	Suggested / Aliased
Total vs Mean	12,271.11	1	12,271.11			
Mean vs Linear	57.82805	4	14.45701	7.852276	0.0003	Suggested
2FI vs Linear	13.27309	6	2.212181	1.283207	0.3114	Aliased
2FI vs Quadratic	2.867418	4	0.716854	0.359775	0.8333	
Cubic vs Quadratic	14.3118	8	1.788975	0.803993	0.6199	
Residual	15.57579	7	2.225113			
Total	12,374.97	30	412.499			

Table 9 Analysis of variance

Source	Sum of squares	df	Mean Square	F value	*P* value prob > F	Significant/Not-significant
Model	57.37	4	14.46	7.85	0.0003	Significant
A- SNPs	0.57	1	0.57	0.31	0.5838	
B-pH	2.39	1	2.39	1.31	0.2656	
C-Contact time	0.30	1	0.30	0.16	0.6892	
D-Alum sol	54.57	1	54.57	29.64	< 0.0001	
Residual	46.03	25	1.84			
Lack of fit	45.62	20	2.28	27.62	0.0008	Not significant
Pure error	0.41	5	0.083			
Cor Total	103.86	29				

Table 10 Predicted and adjusted R-squared

Standard dev.	1.36	R-squared	0.5568
Mean	20.22	Adj R-Squared	0.4859
C. V %	6.71	Pred. R-Squared	0.3185
Press	70.78	Adeq Precision	10.889

The relative effect of contact time and pH on color reduction of wastewater is shown in 3D surface and contour graph in Fig. 8. The graphs show that color reduction is maximum at near neutral pH. If more contact time is provided, with increase in pH, shows lesser reduction in color. It means that both these factors are relatively independent. If same pH is maintained and contact time is increased, then more color reduction can be obtained.

Relative effect of pH and alum solution on color reduction of wastewater is shown in Fig. 9. 3D surface and contour graph show that reduction in color is minimum at more basic conditions and vice versa. Corresponding to 7 pH, 6–7 mL of alum has shown more reduction.

The result in Fig. 10 shows 3D surface and contour graph for relative effect of contact time and alum solution on color reduction of wastewater. It is clear from the graph that color reduction is higher corresponding to 6–7 mL of alum and 2.5–3.5 h of contact time. Increase in alum solution, however, does not further reduce the color of wastewater.

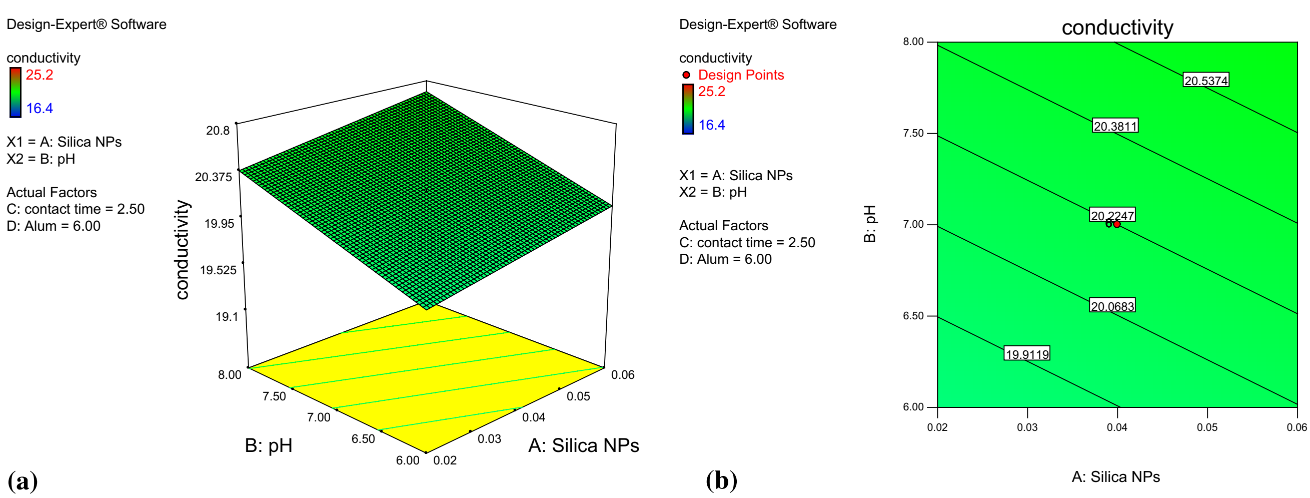

Fig.11 **a** 3D surface and **b** contour graph for relative effect of SNPs and pH on conductivity

Table 11 Sequential model sum of squares for reduction in TDS

Source	Sum of Squares	Df	Mean square	F value	*P* value > F	Suggested / Aliased
Total vs Mean	4415.854	1	4415.854			
Mean vs Linear	21.00044	4	5.250111	7.982048	0.0003	Suggested
Linear vs 2FI	4.642692	6	0.773782	1.245835	0.3276	
2FI vs Quadratic	1.020153	4	0.255038	0.354855	0.8367	
Quadratic vs Cubic	5.212427	8	0.651553	0.819089	0.6105	Aliased
Residual	5.568225	7	0.795461			
Total	4453.298	30	148.4433			

Table 12 Analysis of variance table

Source	Sum of squares	df	Mean square	F value	*P* value > F	Significant/not significant
Model	21.0	4	5.25	7.98	0.0003	Significant
A-SNPs	0.22	1	0.22	0.33	0.5702	
B-pH	0.89	1	0.89	1.35	0.2561a	
C-Contact time	0.12	1	0.12	0.18	0.6757	
D-Alum sol	19.78	1	19.78	30.07	< 0.0001	
Residual	16.44	25	0.66			Not significant
Lack of fit	16.29	20	0.81	27.41	0.0008	
Pure error	0.15	5	0.030			
Cor total	37.44	29				

Table 13 Predicted and adjusted R-squared

Std. Dev.	0.81	R-Squared	0.5609
Mean	12.13	Adj. R-squared	0.4906
C.V. %	6.68	Pred R-squared	0.3247
Press	25.29	Adeq precision	10.967

3.4. Reduction in conductivity

3.4.1. ANOVA for response surface linear model

The Model F-value of 7.85 implies the model is significant. There is only a 0.03% chance that a "Model F-Value" this large could occur due to noise. Values of "Prob > F" less than 0.0500 indicate model terms are significant. In this case D are significant model terms. Values greater than 0.1000 indicate the model terms are not significant (Tables 8 and 9).

The "Pred R-Squared" of 0.3185 is in reasonable agreement with the "Adj R-Squared" of 0.4859 as presented in Table 10.

The final equations for conductivity, in terms of coded and actual are given Eq. 3 & 4, respectively.

Equation in terms of coded factors

$$Conductivity = +20.22 + 0.15 * A + 0.32 * B - 0.11 * C + 1.51 * \tag{3}$$

In this case, A, B, and C are three investigated variables. The impact of each variable in equation is evaluated by the help of *t*-test and *P* values Sharma et al. 2009)).

Equation in terms of actual factors

$$\begin{aligned} Conductivity = &+ 13.37231 + 7.68750 * SNPs + 0.31542 * pH \\ &- 0.074722 * contact\ time + 0.75396 * Alum \end{aligned} \tag{4}$$

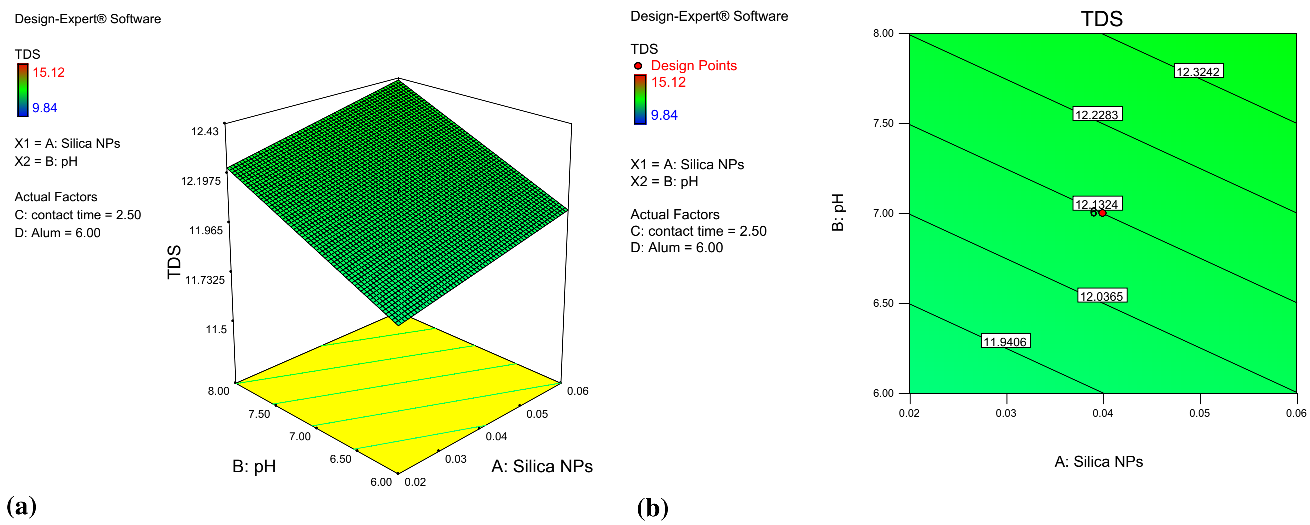

Fig. 12 **a** 3D surface and **b** contour graph for relative effect of SNPs and pH on TDS

Model graphs

The results shown in 3D surface and contour graph in Fig. 11 are for relative effect of SNPs and pH on conductivity of wastewater. The contour graph depicts that conductivity is minimum corresponding to conditions 0.03–0.04 g of silica and 6–7 pH. Higher pH, however, can increase conductivity that might be because of more ionization.

Reduction in TDS

ANOVA for response surface linear model

The Model F-value of 7.98 as shown in Table 10 implies the model is significant. There is only a 0.03% chance that a "Model F-Value" this large could occur due to noise.

Values of "Prob > F" less than 0.0500 indicate model terms are significant. In this case D are significant model terms. Values greater than 0.1000 indicate the model terms are not significant (Tables 11 and 12).

The "Pred R-Squared" of 0.3247 is in reasonable agreement with the "Adj R-Squared" of 0.4906 as showed in Table 13.

The final equations in terms of coded and actual factors are given Eqs. 5 & 6, respectively

$$TDS = +12.13 + 0.095 * A + 0.19 * B - 0.070 * C + 0.91 * D \quad (5)$$

Final Equation in Terms of Actual Factors:

$$TDS = +7.98854 + 4.76250 * SNPs + 0.19242 * pH - 0.046722 * contact\ time + 0.45387 * Alum \quad (6)$$

Model graphs

As linear model was suggested it means that only individual parameters effected the response.

Results for relative effect of SNPs and pH on TDS of wastewater are shown in form of 3D surface and contour graph in Fig. 12. Increase in silica dose has proportional effect on removal of TDS. pH of 6–7 has shown more desired results on TDS reduction.

The results of current study showed that silica nanoparticles along with alum can reduce pollution load significantly. Further investigations can play important role in the purification or desalination of surface water and industrial effluents.

Conclusion

SNPs were synthesized by sol–gel synthesis method. These particles were divided into five main groups on the basis of difference in their calcination temperature ranging from 500 to 900 °C. After synthesis SNPs were characterized by FTIR, UV spectroscopy and XRD. It was observed that SN-3, calcinated at 700 °C showed best results as compared to SN-1, SN-2, SN-4 and SN-5. The parameters were optimized by using response surface methodology (RSM). The maximum reduction was observed corresponding to the conditions: silica dose 0.08 g, pH 7, alum solution 6 mL and contact time of 2.5 h. It can be concluded that SNPs in conjugation with some natural coagulant can reduce pollution load with maximum removal efficiency.

Acknowledgments The authors wish to thank all who assisted in conducting this work.

Funding Author has received no fund from any funding body.

Declarations

Conflict of interest The authors declare that they have no conflict of interest.

References

Ahmad R, Ansari K (2021) Enhanced sequestration of methylene blue and crystal violet dye onto green synthesis of pectin modified hybrid (Pect/AILP-Kal) nanocomposite. Process Biochem 111:132–143

Ahmed S, Ahmad M, Swami BL, Ikram S (2016) A review on plants extract mediated synthesis of silver nanoparticles for antimicrobial applications: a green expertise. J Adv Res 7(1):17–28

Ali A, Zafar MZH, Haq I, Phull AR, Ali JS, Hussain A (2016) Synthesis, characterization, applications, and challenges of iron oxide nanoparticles. Nanotechnol Sci Appl 9:49–49

Atta AM (2020) Novel magnetic silica-ionic liquid nanocomposites for wastewater treatment. Nanomaterials 10(1):71–71

Attinti R, Sarkar D, Barrett KR, Datta R (2015) Adsorption of arsenic (V) from aqueous solutions by goethite/silica nanocomposite. Int J Environ Sci Technol 12(12):3905–3914

Baetke SC, Lammers T, Kiessling F (2015) Applications of nanoparticles for diagnosis and therapy of cancer. Br J Radiol 88(1054):20150207

Baş D, Boyacı IH (2007) Modeling and optimization I: usability of response surface methodology. J Food Eng 78(3):836–845

Basu H, Singhal RK, Pimple MV, Reddy AVR (2015) Arsenic removal from groundwater by goethite impregnated calcium alginate beads. Water Air Soil Pollution 226(2):1–11

Bettermann P, Liebau F (1975) The transformation of amorphous silica to crystalline silica under hydrothermal conditions. Contrib Miner Petrol 53(1):25–36

Ealias AM, Saravanakumar M (2017) A review on the classification, charac- terisation, synthesis of nanoparticles and their application. Mater Sci Eng 263:32019–32019

Gita S, Hussan A, Choudhury TG (2017) Impact of textile dyes waste on aquatic environments and its treatment. Environ Ecol 35(3C):2349–2353

Heidi Lynn R, Priscilla BLG, Emmanuel I (2012) Metal nanoparticle modified polysulfone membranes for use in wastewater treatment: a critical review. Journal of surface engineered materials and advanced technology

Irfan M, Siddiqui M, Bashir F, Butt M, Abbas N (2020) Efficient removal of hydrogen sulfide from wastewater using waste-tire-derived rubber particles. Int J Environ Sci Technol 17(7):3515–3524

Kandpal D, Kalele S, Kulkarni S (2007) Synthesis and characterization of silica-gold core-shell (SiO 2@ Au) nanoparticles. Pramana 69(2):277–283

Khan NA, Khan SU, Ahmed S, Farooqi IH, Dhingra A, Hussain A, Changani F (2019) Applications of nanotechnology in water and wastewater treatment: a review. Asian J Water Environ Pollut 16(4):81–86

Li X, Iocozzia J, Chen Y, Zhao S, Cui X, Wang W, Lin Z (2018) From precision synthesis of block copolymers to properties and applications of nanoparticles. Angew Chem Int Ed 57(8):2046–2070

Merci S (2020) Investigation of photocatalytic chlorpyrifos degradation by a new silica mesoporous material immobilized by WS2 and Fe3O4 nanoparticles: Application of response surface methodology. Appl Organomet Chem 34(3):e5343–e5343

Mittala J, Ahmadb R, Mittalc A (2021) Kahwa tea (Camellia sinensis) carbon—a novel and green low-cost adsorbent for the sequestration of Titan yellow dye from its aqueous solutions. Desalinat Water Treat 227:404–411

Mohammadi M, Khorrami MK, Ghasemzadeh H (2019) ATR-FTIR spec- troscopy and chemometric techniques for determination of polymer solution viscosity in the presence of SiO2 nanoparticle and salinity. Spectrochim Acta Part A Mol Biomol Spectrosc 220:117049–117049

Mohammed L, Gomaa HG, Ragab D, Zhu J (2017) Magnetic nanoparticles for environmental and biomedical applications: A review. Particuology 30:1–14

Morin-Crini N (2019) Synthesis of silica materials containing cyclodextrin and their applications in wastewater treatment. Environ Chem Lett 17(2):683–696

Mourdikoudis S, Pallares RM, Thanh NT (2018) Characterization techniques for nanoparticles: comparison and complementarity upon studying nanoparticle properties. Nanoscale 10(27):12871–12934

Nandanwar R, Singh P, Haque FZ (2015) Synthesis and characterization of SiO2 nanoparticles by sol-gel process and its degradation of methylene blue. Am Chem Sci J 5(1):1–10

Naseem T, Durrani T (2021) The role of some important metal oxide nanoparticles for wastewater and antibacterial applications: a review. Environ Chem Ecotoxicol 3:59–75

Olawale O, Oyawale FA (2012) Characterization of rice husk via atomic absorption spectrophotometer for optimal silica production. Int J Sci Technol 2(4):210–213

Ong CB, Ng LY, Mohammad AW (2018) A review of ZnO nanoparticles as solar photocatalysts: synthesis, mechanisms and applications. Renew Sustain Energy Rev 81:536–551

Prasad T, Halder S, Dhar S (2020) Process parameter effects on particle size reduction of sol-gel synthesized silica nanoparticles. Materials Today: Proceed 22:1669–1675

Ramimoghadam D, Bagheri S, Hamid SB (2014) Biotemplated synthesis of anatase titanium dioxide nanoparticles via lignocellulosic waste material. BioMed Res Int 2014:1–7

Rovani S, Santos JJ, Corio P, Fungaro DA (2018) Highly pure silica nanoparti- cles with high adsorption capacity obtained from sugarcane waste ash. ACS Omega 3(3):2618–2627

Sharma P, Singh L, Dilbaghi N (2009) Response surface methodological approach for the decolorization of simulated dye effluent using Aspergillus fumigatus fresenius. J Hazard Mater 161(2–3):1081–1086

Singh S (2019) Applications of nanoparticles in wastewater treatment. Nanobiotechnol Bioformulat, 395–418

Soni G, Yadav KS (2015) Applications of nanoparticles in treatment and diagnosis of leukemia. Mater Sci Eng, C 47:156–164

Stanley R, Nesaraj AS (2014) Effect of surfactants on the wet chemical synthesis of silica nanoparticles. Int J Appl Sci Eng 12(1):9–21

Stark WJ, Stoessel PR, Wohlleben W, Hafner A (2015) Industrial applications of nanoparticles. Chem Soc Rev 44(16):5793–5805

Wyckoff RW (1925) Crystal structure of high temperature cristobalite. Am J Sci 5(54):448–459

Xu HY, Qi SY, Li Y, Zhao Y, Li JW (2013) Heterogeneous Fenton-like discoloration of Rhodamine B using natural schorl as catalyst:

optimization by response surface methodology. Environ Sci Pollut Res 20(8):5764–5772
Xue SH, Xie H, Ping H, Li QC, Su BL, Fu ZY (2015) Induced transformation of amorphous silica to cristobalite on bacterial surfaces. RSC Adv 5(88):71844–71848
Zazo H, Colino CI, Lanao JM (2016) Current applications of nanoparticles in infectious diseases. J Control Release 224:86–102
Zhang Y (2011) Synthesis of mesoporous carbon capsules encapsulated with magnetite nanoparticles and their application in wastewater treatment. J Mater Chem 21(11):3664–3671
Zhu Y, Liao L (2015) Applications of nanoparticles for anticancer drug delivery: a review. J Nanosci Nanotechnol 15(7):4753–4773